

MODELLING OF LAMINATED GLASS INTERLAYER BY FRACTIONAL VISCOELASTICITY

BARBORA HÁLKOVÁ*, JAROSLAV SCHMIDT

Czech Technical University in Prague, Faculty of Civil Engineering, Department of Mechanics, Thákurova 7, 166 29 Prague 6, Czech Republic

* corresponding author: barbora.halkova@fsv.cvut.cz

ABSTRACT. Fractional calculus, i.e. the theory of derivatives and integrals of non-integer order, can be efficiently used for the theoretical modelling of viscoelastic materials. Our research is focused on the polyvinyl butyral which is used as an interlayer for the laminated glass. Polyvinyl butyral can be classified as a viscoelastic material and the introduction of the fractional viscoelasticity seems to be appropriate tool for its description. This paper briefly introduces the springpot element and its connection into more complex theoretical models. We mainly consider the generalized Maxwell model in its standard and fractional form and show their application by fitting the data obtained by experimental analysis.

KEYWORDS: Laminated glass, polymer interlayer, theory of viscoelasticity, fractional viscoelasticity, springpot, generalized Maxwell model, fractional calculus, storage modulus.

1. INTRODUCTION

Laminated glass, see [1], is a composite material, which consists of a solid glass plates (float, toughened, tempered glass or their combination) and interlayers made of polymers (mostly the polyvinyl butyral, which will be also considered in the following text) or cast resins. The interlayer has primarily the safety function, it improves the post-breakage behaviour of the glass elements. It also ensures interaction between the main load-bearing glass plates, its effect is mostly important in the case of bending, when the interlayer directly affects the stiffness of the cross section and is mostly stressed by shear.

The polyvinyl butyral (PVB) type of interlayer can be classified as a viscoelastic material [2]. Its behaviour is somewhere between purely elastic and purely viscous. The viscoelastic behaviour is time and load-history dependent, phenomenon such as creep and relaxation are significant. For the accurate description of the viscoelastic material we need to use more complex theoretical models, while the ideal elasticity and viscosity stand for the limit cases, see [3] for broader description.

2. VISCOELASTICITY

The standard theory of viscoelasticity commonly uses the theoretical models composed of elastic and viscous elements (springs and dashpots). The fractional viscoelasticity, see [4], applies the principles of fractional calculus and introduces another rheological element, the springpot. However, the fractional calculus is not discussed in detail here because it is out of scope of this article and the interested reader is referred to [5].

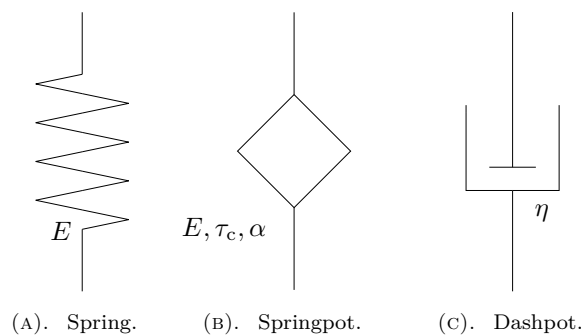


FIGURE 1. Rheological scheme of spring, springpot and dashpot.

The linear spring (see Figure 1a) is a rheological element, which represents ideally elastic behaviour of the material. The constitutive law, also known as Hooke's law, has the following form:

$$\sigma(t) = E\varepsilon(t), \quad (1)$$

where

σ stands for the stress,

ε for the strain,

E for Young's modulus of elasticity.

The stress is a linear function of the strain.

The viscous damper (dashpot) On the other hand, the viscous damper (dashpot) (see Figure 1c) represents the model of ideally viscous fluid. The stress is directly proportional to the strain rate (i.e. to the first derivative of the strain). The constitutive law, also known as Newton's equation of viscosity, has the following form:

$$\sigma(t) = \eta \dot{\varepsilon}(t), \quad (2)$$

where

η stands for the coefficient of viscosity,

$\dot{\varepsilon}$ the time derivative of the strain.

The springpot (see Figure 1b) then represents a transition between the two cases mentioned above. Fractional viscoelasticity, see [4], assumes the constitutive law in the following form:

$$\sigma(t) = \xi D^\alpha \varepsilon(t), \quad (3)$$

where

ξ and α are parameters of the springpot,

D^α denotes the α -th time derivative.

The point of fractional viscoelasticity is to assume α as non-integer.

We have already mentioned that the ideal elasticity and ideal viscosity stands for the limit cases of viscoelastic behaviour, therefore we can define the limit cases for the springpot parameters and consider α only in the interval $\langle 0, 1 \rangle$.

When we introduce the characteristic time τ_c in the following form:

$$\tau_c = \frac{\eta}{E}, \quad (4)$$

Equation (3) can be rewritten as:

$$\sigma(t) = E \tau_c^\alpha D^\alpha \varepsilon(t). \quad (5)$$

The replacement of ξ by $E \tau_c^\alpha$ better illustrates the physical meaning of the constant ξ in the limit cases. For $\alpha = 0$ we receive:

$$\sigma(t) = E \frac{d^0 \varepsilon(t)}{dt^0} = E \varepsilon(t), \quad (6)$$

describing purely elastic response, remind Equation (1). We see that in this limit the parameter ξ is equal to the modulus of elasticity E and the behaviour of the springpot corresponds to the behaviour of an elastic element. On the other hand, for $\alpha = 1$ we receive:

$$\sigma(t) = E \tau_c \frac{d\varepsilon(t)}{dt} = \eta \dot{\varepsilon}(t). \quad (7)$$

In this limit case the behaviour of the springpot corresponds to the behaviour of the viscous element (remind Equation (2)), while the constant ξ become the constant of viscosity η .

2.1. RELAXATION MODULUS OF SPRINGPOT

The relaxation is the phenomenon where the stress gradually decreases over time even if the strain remains constant. On the other hand, the creep can be explained as a phenomenon where the the strain gradually increases over time while the stress remains

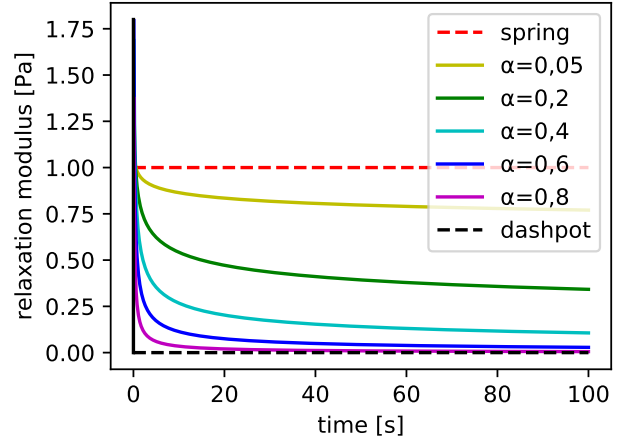


FIGURE 2. Relaxation modulus of a springpot according to different values of α .

constant, for the broader description of these phenomena see [3]. In the following text we focus on the relaxation mode only, because it can be more easily interpreted in connection with the results of our experimental analysis.

Relaxation modulus of the material is defined as the stress response to the Heaviside strain load:

$$\varepsilon(t) = H(t), \quad (8)$$

unit-value strain load which is applied instantaneously in time $t = 0$ and remains constant for times $t > 0$.

In the case of the springpot element we consider the fractional derivative D^α as the Riemann-Liouville type of derivative, see [6]. The resulting relaxation modulus has the following form:

$$R(t) = \frac{E}{\Gamma(1-\alpha)} \left(\frac{t}{\tau_c} \right)^{-\alpha} H(t), \quad (9)$$

where

Γ denotes the Gamma function.

Figure 2 shows the relaxation modulus of a springpot according to different values of α , while the dashed lines represent the limit cases given by elastic and viscous behaviour.

2.2. SPRINGPOT UNDER HARMONIC LOAD

As a part of our research the experimental analysis of the laminated glass is provided as well. The samples are loaded by a harmonic torque. Therefore we are interested in the behaviour of theoretical models under the harmonic load as well.

The prescribed strain load and the corresponding stress response have the following forms:

$$\begin{aligned} \varepsilon^*(\omega) &= \varepsilon_0^* e^{i\omega t}, \\ \sigma^*(\omega) &= \sigma_0^* e^{i\omega t}, \end{aligned} \quad (10)$$

where

ε_0^* and σ_0^* are the amplitudes of the harmonic strain and stress in the complex plane,

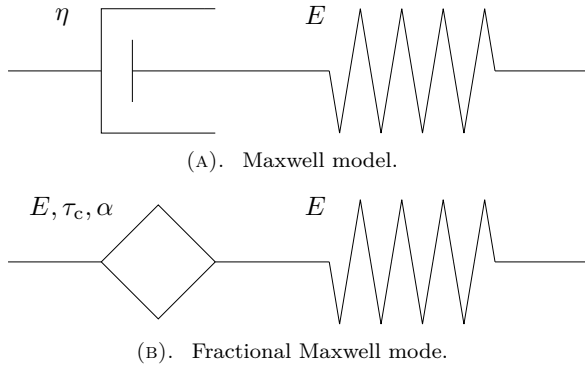


FIGURE 3. Rheological scheme of the Maxwell model and the fractional Maxwell model.

e is the Euler constant,
 i is the imaginary unit.

The complex modulus E^* can now be defined as:

$$E^*(\omega) = \frac{\sigma_0^*}{\varepsilon_0^*}. \quad (11)$$

If we separate the real part of the complex modulus, we receive the storage modulus E' which corresponds to the elastic part of the response. On the other hand, the imaginary part, the loss modulus E'' represents the viscous part of the response. In the following text we focus on the storage modulus due to better accuracy with which the storage modulus is obtained from experiments.

The complex modulus of the springpot element is written as:

$$E^*(\omega) = E(i\omega\tau_c)^\alpha. \quad (12)$$

The storage modulus is then obtained by separating the real part of the complex modulus as:

$$E'(\omega) = \text{Re}(E^*) = E(\omega\tau_c)^\alpha \cos\left(\alpha\frac{\pi}{2}\right). \quad (13)$$

2.3. THEORETICAL MODELS

To improve the description of the viscoelastic behaviour, the rheological elements can be arranged together in series or in parallel to create more accurate models. The overview of some theoretical models can be found for example in [7], while here we limit attention to those, which seem to be appropriate for the description of the PVB interlayer.

Maxwell cell is a serial connection of an elastic spring and a viscous dashpot. By the replacement of the viscous element with the springpot we obtain the fractional Maxwell cell. Both rheological schemes with the variable parameters of each element are shown in Figure 3. The relaxation moduli of the Maxwell cell and the fractional Maxwell cell are respectively:

$$R(t) = Ee^{-t/\tau_c}H(t), \quad (14)$$

$$R(t) = EE_{\alpha,1}\left(-\left(\frac{t}{\tau_c}\right)^\alpha\right)H(t), \quad (15)$$

where

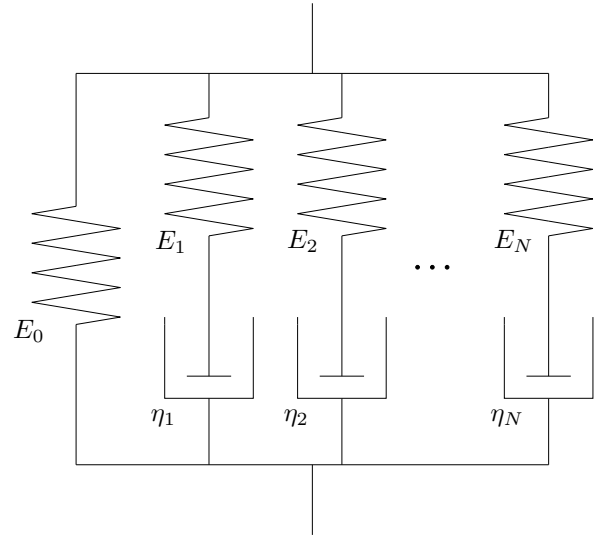


FIGURE 4. Rheological scheme of the generalized Maxwell model.

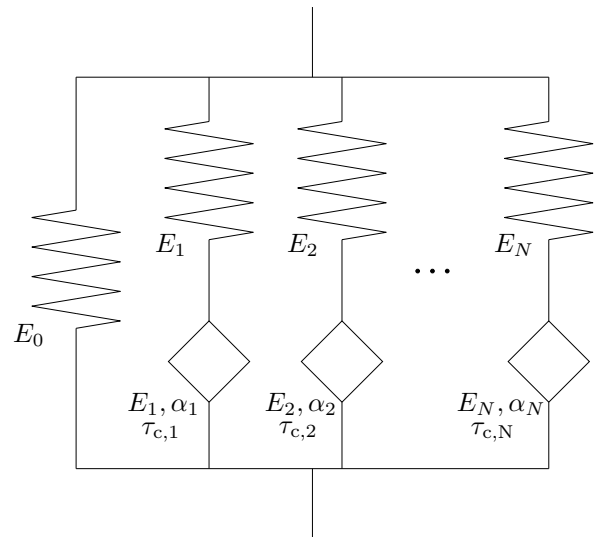


FIGURE 5. Rheological scheme of the fractional Maxwell chain.

$E_{\alpha,1}$ is the Mittag-Leffler function.

For the limit case $\alpha = 1$ it holds that $E_{1,1}(x) = e^x$, see [8], and therefore Equation (14) and Equation (15) become identical in this limit case.

The storage moduli of the Maxwell cell and the fractional Maxwell cell are then:

$$E'(\omega) = E\frac{\omega^2\tau_c^2}{\omega^2\tau_c^2 + 1}, \quad (16)$$

$$E'(\omega) = E\frac{(\tau_c\omega)^{2\alpha} + (\tau_c\omega)^\alpha \cos(\alpha\frac{\pi}{2})}{(\tau_c\omega)^{2\alpha} + 2(\tau_c\omega)^\alpha \cos(\alpha\frac{\pi}{2}) + 1}. \quad (17)$$

Generalized Maxwell model (also known as the Maxwell chain) is the parallel connection of a spring and N Maxwell cells, see Figure 4.

The fractional Maxwell chain is then obtained as a parallel connection of a spring and N fractional Maxwell cells, see the rheological scheme in Figure 5.

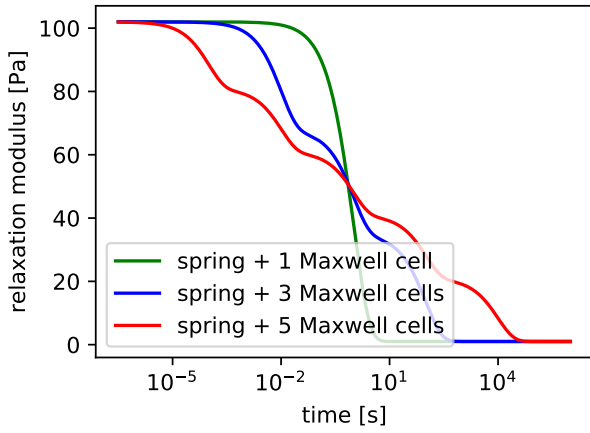


FIGURE 6. Relaxation modulus of the Maxwell chain compare to the number of cells.

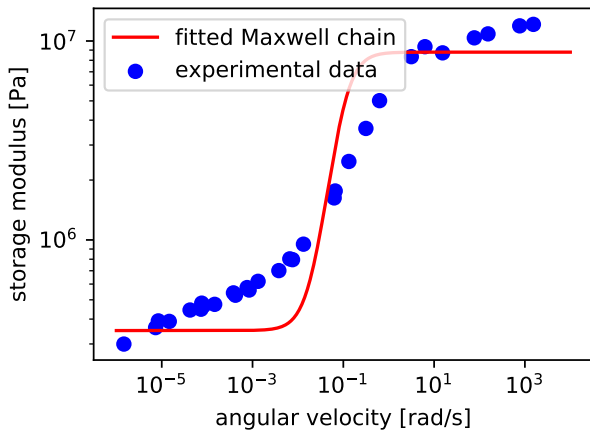


FIGURE 7. Fitting experimental data of G' to 1-cell Maxwell chain.

The parallel connection of the cells in the generalized model enables us to obtain the relaxation modulus of the Maxwell (resp. the fractional Maxwell) chain superpositionally. The same applies to the storage modulus. The relaxation modulus and the storage modulus of the generalized models have the following form:

$$R(t) = E_0 + \sum_{i=1}^n R_i, \quad (18)$$

$$E'(t) = E_0 + \sum_{i=1}^n E'_i, \quad (19)$$

where

E_0 is the Young modulus of elasticity of the spring,

R_i are the relaxation moduli,

E'_i the storage moduli of each of the Maxwell (resp. the fractional Maxwell) cells.

It is obvious that the behaviour of these generalized models depends on the number of the Maxwell (resp. the fractional Maxwell) cells connected together. This is illustrated in Figure 6 which shows the difference in the relaxation modulus of a standard Maxwell chain with 1, 3 and 5 connected Maxwell cells.

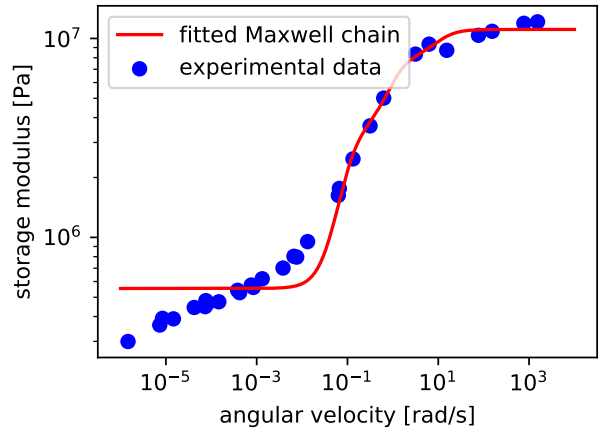


FIGURE 8. Fitting experimental data of G' to 3-cell Maxwell chain.

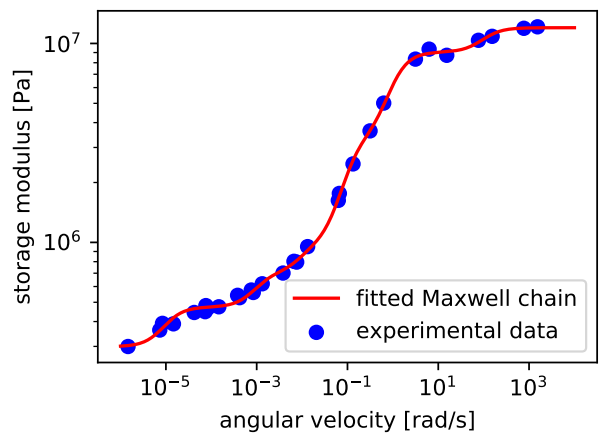


FIGURE 9. Fitting experimental data of G' to 7-cell Maxwell chain.

2.4. VALIDATION OF THEORETICAL MODELS

Each of the theoretical models has the finite amount of unknown parameters (moduli of elasticity E , characteristic times τ_c , viscosities η or the springpot parameters α). These parameters occur in analytical equations prescribing the behaviour of the models, e.g. the relaxation modulus.

For our research the data obtained by experiments performed on laminated glass presented in [9] were used. The validation of the theoretical models was provided by fitting the parameters of the storage modulus. The Python optimization tool from SciPy was used for fitting the parameters, this tool uses the method of non-linear least squares to fit the analytical function to experimental data. The results are displayed in the following figures, where the blue dots illustrate the experimentally obtained data while the red curve is the fitted analytical solution.

Figure 7 shows the approximation by the 1-cell Maxwell chain. However, the approximation is not very accurate. To improve the accuracy we need to add more Maxwell cells to the generalized model. The increase of the number of Maxwell cells from 1 to 3 is shown in Figure 8. The approximation is good on the wider range of frequencies. As is shown in Figure 9, the

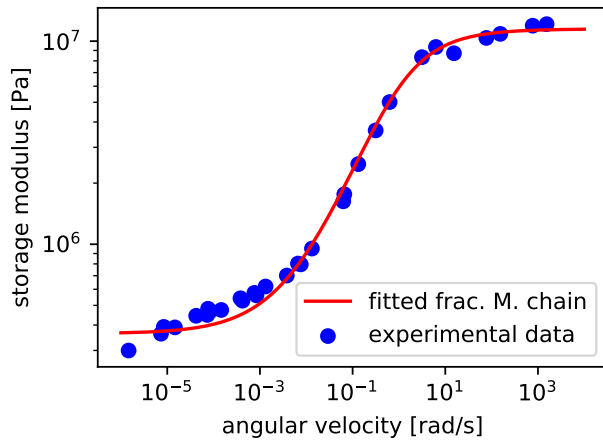


FIGURE 10. Fitting experimental data of G' to 1-cell fractional Maxwell chain.

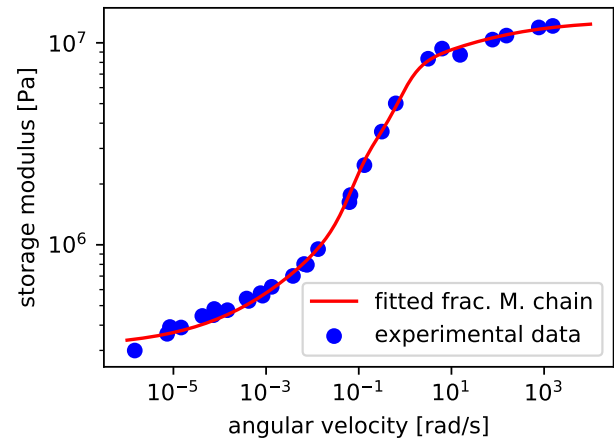


FIGURE 12. Fitting experimental data of G' to 3-cell fractional Maxwell chain.

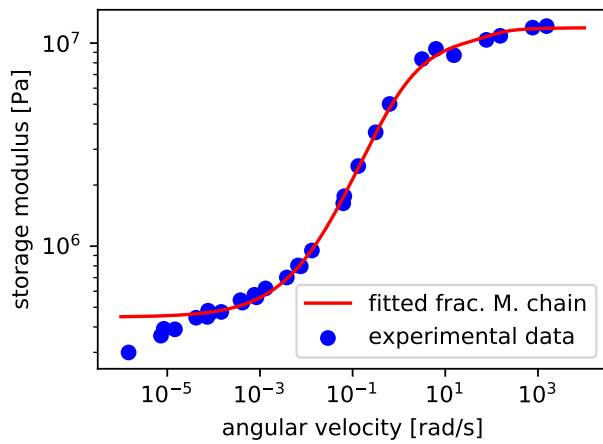


FIGURE 11. Fitting experimental data of G' to 2-cell fractional Maxwell chain.

7-cells Maxwell chain approximates the experimental data well in the whole measured frequency range. On the other hand, the increase of the number of the cells from 1 to 7 also significantly increases the number of the unknown parameters that need to be fitted.

The approximation by the fractional Maxwell chain is shown in Figures 10–12. Even for the 1-cell fractional Maxwell chain (Figure 10) the accuracy of the approximation is significantly better compare to standard 1-cell Maxwell chain (Figure 7). However, the accuracy can also be improved by adding more fractional Maxwell cells. Figure 11 shows approximation by the 2-cells and Figure 12 the 3-cells fractional Maxwell chain. In the last mentioned case we can talk about almost perfect fit to the experimental data.

The fractional Maxwell chain shows one more significant advantage. While the curve of the standard Maxwell chain become horizontal on the edges of the measured domain, the fractional Maxwell chain still shows the growing trend of the curve. Therefore, the fractional Maxwell chain might be used for data extrapolation outside the experimentally measured domain.

This section clearly shows the results that the frac-

tional Maxwell chain can provide better approximations of the experimental data in comparison to standard generalized Maxwell model. Also it can be used for the data extrapolation for which the standard Maxwell chain is not suitable. Therefore the use of the fractional models might be beneficial despite their disadvantages which lie in the need of the more difficult mathematical apparatus.

3. CONCLUSION

Fractional viscoelasticity seems to be an efficient tool to describe the behaviour of a polyvinyl butyral, the material of the interlayer of laminated glass. The principles of fractional calculus are introduced together with the springpot element. This rheological element can be used in connections with springs or dashpots to make more complex theoretical models. For our applications, the generalized Maxwell chain models presented in its standard and fractional forms are sufficiently accurate and effective, particularly when considering the approximation of the experimental data.

Comparing both formulations, the fractional viscoelasticity requires a complex mathematical apparatus to calculate derivatives and integrals of non-integer order. On the other hand, by the use of fractional models the number of the fitted parameters may be reduced in compare to standard viscoelastic models. On top of that, it allows for extrapolation of data outside the experimentally measured domain. Therefore, the fractional model can be directly exploited in fitting the experimentally measured master curve very accurately adopting a few parameters only. This smooth approximation can be in turn used in calibrating the Maxwell chain model typically adopted in finite element simulations as implementation of the fractional model in the framework of the finite element method is still a subject of an ongoing research.

ACKNOWLEDGEMENTS

This publication was supported by the Czech Science Foundation, the grant No. 22-15553S and by the Grant Agency of the Czech Technical University in Prague, grant No. SGS22/031/OHK1/1T/11.

REFERENCES

- [1] W. Laufs, A. Luible. Introduction on use of glass in modern buildings. Tech. rep., EPFL, Laboratoire de la construction métallique ICOM, 2003.
- [2] M. Haldimann, A. Luible, M. Overend. *Structural use of glass*, vol. 10 of *Structural Engineering Documents*. Iabse, Zürich, 2008. ISBN 978-3-85748-119-2. <https://doi.org/10.2749/sed010>
- [3] M. Jirásek, J. Zeman. *Přetváření a porušování materiálů: dotvarování, plasticita, lom a poškození*. České vysoké učení technické v Praze, Prague, 2006. ISBN 978-80-01-05064-4.
- [4] R. C. Koeller. Applications of fractional calculus to the theory of viscoelasticity. *Journal of Applied Mechanics* **51**(2):299–307, 1984. <https://doi.org/10.1115/1.3167616>
- [5] F. Mainardi, R. Gorenflo. Fractional calculus and special functions, 2013. Lecture Notes On Mathematical Physics.
- [6] R. L. Graham, D. E. Knuth, O. Patashnik, S. Liu. Concrete mathematics: a foundation for computer science. *Computers in Physics* **3**(5):106–107, 1989. <https://doi.org/10.1063/1.4822863>
- [7] B. Hálková. *Viscoelastic description of polymer interlayer of laminated glass*. Bachelor's thesis, České vysoké učení technické v Praze, Prague, 2022. [2022-08-15]. <https://dspace.cvut.cz/handle/10467/102633>
- [8] R. Gorenflo, F. Mainardi, S. Rogosin. Mittag-leffler function: properties and applications. In *Volume 1 Basic Theory*, pp. 269–296. De Gruyter, Berlin, Boston, 2019. <https://doi.org/10.1515/9783110571622-011>
- [9] T. Hána, T. Janda, J. Schmidt, et al. Experimental and numerical study of viscoelastic properties of polymeric interlayers used for laminated glass: Determination of material parameters. *Materials* **12**(14):2241, 2019. <https://doi.org/10.3390/ma12142241>